ADVANCES IN ATMOSPHERIC SCIENCES, VOL. 26, NO. 2, 2009, 293–304

Nonlinear Feature of the Abrupt Transitions between Multiple Equilibria States of an Ecosystem Model

SUN Guodong*[1,2] (孙国栋) and MU Mu[1] (穆 穆)

[1] *State Key Laboratory of Numerical Modeling for Atmospheric Sciences and Geophysical Fluid Dynamics, Institute of Atmospheric Physics, Chinese Academy of Sciences, Beijing* 100029

[2] *Graduate University of Chinese Academy of Sciences, Beijing* 100049

(Received 1 November 2007; revised 27 February 2008)

ABSTRACT

Based on a five-variable theoretical ecosystem model, the stability of equilibrium state and the nonlinear feature of the transition between a grassland state and a desert state are investigated. The approach of the conditional nonlinear optimal perturbations (CNOPs), which are the nonlinear generalization of the linear singular vectors (LSVs), is adopted. The numerical results indicate that the linearly stable grassland and desert states are nonlinearly unstable to large enough initial perturbations on the condition that the moisture index μ satisfies $0.3126 < \mu < 0.3504$. The perturbations represent some kind of anthropogenic influence and natural factors. The results obtained by CNOPs, LSVs and Lyapunov vectors (LVs) are compared to analyze the nonlinear feature of the transition between the grassland state and the desert state. Besides this, it is shown that the five-variable model is superior to the three-variable model in providing more visible signals when the transitions occur.

Key words: nonlinear feature, abrupt transition, grassland and desert ecosystem, shading effect

Citation: Sun, G. D., and M. Mu, 2009: Nonlinear feature of the abrupt transitions between multiple equilibria states of an ecosystem model. *Adv. Atmos. Sci.*, **26**(2), 293–304, doi: 10.1007/s00376-009-0293-8.

1. Introduction

The grassland ecosystem is a complicated open system. There exist different equilibria (e.g., grassland, desert, etc.) at various spatial and temporal scales due to climate conditions (temperature, precipitation, etc.) in grassland ecosystems. Transitions often occur between the different equilibria states in the semi-arid areas. For example, in Inner Mongolia, China, the boundary between the grassland and the desert is sharp and rough along the line of a moisture index of 0.3, which is the ratio of annual precipitation to potential evaporation (Zeng et al., 2004). There also exist the transitions from the tropical rain-forest to the sandy desert of the Sahara (Zeng, 2003). Quite a few of researchers have studied the abrupt desertification in the temporal scale, especially in the mid-Holocene in north Africa, both with a complex model (Claussen, 1997, 1998; Claussen et al., 1999) and with a simple Zeng-Neelin model (Zeng et al., 2002; Liu et al., 2006).

In order to study the grassland ecosystem, some models have been built (Klausmeier, 1999; Sitch et al., 2003; Zeng et al., 1994; Li et al., 2004). Among these ecosystem models, the simple ecological-hydrological models are prominent (Zeng and Zeng, 1996a,b; Zeng et al., 2003, 2004, 2005a,b,c, 2006). In spite of the simplicity, the models could clearly and compactly reveal the essential features of the complex system of atmosphere-ecosystem-soil, such as multi-equilibria, bifurcation and abrupt changes. Zeng et al. (2004) indicated the multiple equilibria potentially exist in the moisture index around 0.3, in good agreement with the observation data in Inner Mongolia, China. In addition, it was shown that "shading effect" of the living canopy and the wilted biomass might be one of the major mechanisms leading to the desertification over a relatively short period.

This paper aims to analyze the stability of the grassland ecosystem and the nonlinear feature of the transition between the grassland state and the desert

*Corresponding author: SUN Guodong, sungd@mail.iap.ac.cn

state with a theoretical model. In past researches, a linear method is applied to analyze the stability of the ecosystem (Zeng et al., 2005c). However, the ecosystem is a nonlinear system, and a large enough disturbance can result in a transition from one state to another (Zeng and Zeng, 1996b). It is deficient to analyze the stability of the equilibrium state by the linear approximation. To analyze the stability of the nonlinear ecosystem, conditional nonlinear optimal perturbations (CNOPs), which are the nonlinear generation of the linear singular vectors (LSVs), are applied. CNOPs are a new approach to study nonlinear problems (Mu et al., 2003), and have been applied to investigate the dynamics of ENSO predictability, prediction error (Mu and Duan, 2003; Duan et al., 2004) and the nonlinear stability of steady states of the thermohaline circulation (Mu et al., 2004; Sun et al., 2005).

In Mu and Wang's work (2007), they analyzed the stability of a grassland ecosystem with a three-variable model. Furthermore, we will analyze the stability of ecosystem equilibrium state with a five-variable model. It is found that there is a nonlinear feature with respect to the transition induced by CNOPs, LSVs, and Lyapunov vectors (LVs), and that the five-variable model is superior to the three-variable model in providing detectable signals when the transition occurs.

2. The model and the CNOPs

2.1 *Model*

To analyze the stability of the grassland ecosystem, a simple ecosystem model is adopted. The five-variable ecosystem model consists of a three-variable ecosystem model and a three-layer land surface hydrological model, and deals with one species of grass (Zeng et al., 2003, 2005c). The variables of the model are living biomass (M_c), wilted biomass (M_d), water content in vegetation canopy (W_c), water content in thin surface layer of soil (W_s) and water content in rooting layer (W_r). The variables satisfy

$$\frac{dM_\mathrm{c}}{dt}=\alpha^*[G(M_\mathrm{c},W_\mathrm{r})-D_\mathrm{c}(M_\mathrm{c},W_\mathrm{r})-C_\mathrm{c}(M_\mathrm{c})]\,, \quad (1a)$$

$$\frac{dM_\mathrm{d}}{dt}=\alpha^*[\beta' D_\mathrm{c}(M_\mathrm{c},W_\mathrm{r})-D_\mathrm{d}(M_\mathrm{d})-C_\mathrm{d}(M_\mathrm{d})]\,, \quad (1b)$$

$$\frac{dW_\mathrm{c}}{dt}=P_\mathrm{c}(M_\mathrm{c})+E_\mathrm{r}(M_\mathrm{c},W_\mathrm{r})-E_\mathrm{c}(M_\mathrm{c},W_\mathrm{r})-R_\mathrm{c}(M_\mathrm{c})\,, \quad (1c)$$

$$\frac{dW_\mathrm{s}}{dt}=P_\mathrm{s}(M_\mathrm{c})-E_\mathrm{s}(M_\mathrm{c},W_\mathrm{s},M_\mathrm{d})+R_\mathrm{c}(M_\mathrm{c})-Q_\mathrm{sr}(W_\mathrm{s},W_\mathrm{r})-R_\mathrm{s}(M_\mathrm{c},W_\mathrm{s},M_\mathrm{d})\,, \quad (1d)$$

$$\frac{dW_\mathrm{r}}{dt}=P_\mathrm{r}(M_\mathrm{c})+\alpha_\mathrm{r}R_\mathrm{s}(M_\mathrm{c},W_\mathrm{s},M_\mathrm{d})-E_\mathrm{r}(M_\mathrm{c},W_\mathrm{r})+Q_\mathrm{sr}(W_\mathrm{s},W_\mathrm{r})-R_\mathrm{r}(M_\mathrm{c},W_\mathrm{r})\,. \quad (1e)$$

According to the hypotheses proposed by Zeng et al. (2003, 2004, 2005c), the equation of vegetation canopy becomes

$$P_\mathrm{c}(M_\mathrm{c})+E_\mathrm{r}(M_\mathrm{c},W_\mathrm{r})-E_\mathrm{c}(M_\mathrm{c},W_\mathrm{r})=0\,. \quad (2)$$

Thus, Eqs. (1a), (1b), (1d) and (1e) form a new set of ordinary differential equations (ODEs), where terms $M_\mathrm{c}=x\tilde{x}, M_\mathrm{d}=z\tilde{z}, W_\mathrm{s}=y_1\tilde{y_1}$, and $W_\mathrm{r}=y_2\tilde{y_2}$; dimensional constants $\tilde{x}$, $\tilde{y_1}$, $\tilde{y_2}$ and $\tilde{z}$ are the corresponding characteristic values. In Eq. (1), some expressions established by Zeng et al. (2004, 2006) are adopted. However, some expressions are not explicitly shown yet, such as R_r, etc.. In the Appendix A, these expressions will be given in detail.

2.2 *Conditional nonlinear optimal perturbations*

For the benefit of the readers, we will introduce the approach of CNOPs established by Mu et al. (2003). Let M_τ be the propagator of the five-variable ecosystem model from initial time 0 to τ. $\boldsymbol{U}(\tau)=(x_\tau, y_{1\tau}, y_{2\tau}, z_\tau)$ is a solution to the nonlinear equations and satisfies $\boldsymbol{U}(\tau)=M_\tau(\boldsymbol{U}_0)$. $\boldsymbol{U}_0=(x_0, y_{10}, y_{20}, z_0)$ is the initial value of the living biomass, the soil moisture of the surface layer and root zone, and the wilted biomass.

For a proper norm $\|\cdot\|$, an initial perturbation $\boldsymbol{u}_{0\delta}$ is called a CNOP if and only if

$$J(\boldsymbol{u}_{0\delta})=\max_{\|\boldsymbol{u}_0\|\leqslant\delta} J(\boldsymbol{u}_0)\,, \quad (3)$$

where

$$J(\boldsymbol{u}_0)=\|M_\tau(\boldsymbol{U}_0+\boldsymbol{u}_0)-M_\tau(\boldsymbol{U}_0)\|\,, \quad (4)$$

and $\|\boldsymbol{u}_0\|\leqslant\delta$ is the initial constraint condition. The CNOPs are the initial perturbations whose nonlinear evolution attains the maximal value of the functional J at time τ. That is to say, the CNOPs are the global maximum of the objective function J.

The constraint condition must be physically reasonable. For the five-variable ecosystem model, the values of the living biomass, the soil moisture of the surface layer and root zone and the wilted biomass are nonnegative. Therefore, the initial perturbation should satisfy

$$x_0+\delta x\geqslant 0\,,\ \ y_{10}+\delta y_1\geqslant 0\,,$$
$$y_{20}+\delta y_2\geqslant 0\,,\ \ z_0+\delta z\geqslant 0\,, \quad (5)$$

where $(x_0, y_{10}, y_{20}, z_0)$ is $\boldsymbol{U}_0$, and $(\delta x, \delta y_1, \delta y_2, \delta z)$ is $\boldsymbol{u}_0$ in Eq. (3).

The ODEs are solved by a fourth-order Runge-Kutta method with a time step $dt = 1/24$ (representing half of a month). The sequential quadratic programming (SQP) solver is adopted to calculate CNOPs. The details of the SQP can be found in Mu et al. (2003).

3. Nonlinear stability analysis

To analyze the stability of the grassland ecosystem, the multiple equilibrium states are first presented in Fig. 1 with the five-variable model. The results are similar to those of Zeng et al. (2005c, Fig. 6).

Here, two different equilibrium states A ($x = 0.538$, $y_1 = 0.647$, $y_2 = 0.629$, $z = 0.567$) and B ($x = 0.000$, $y_1 = 0.383$, $y_2 = 0.415$, $z = 0.000$), which are the linearly stable grassland and desert equilibria states respectively, are chosen under the condition of the moisture index μ being 0.32.

3.1 *Nonlinear stability analysis of grassland state A*

To investigate the stability of the equilibrium state A, the CNOPs are calculated under different constraints radii (Table 1). We also point out that for CNOPs the results for $\tau = 10$ years are similar to those for $\tau = 20$ years, so we only present the former. The model is integrated with the initial values being the CNOPs superposed on the basic state A. The results are shown in Fig. 2.

Figure 2 shows that the grassland ecosystem will finally recover to the grassland state A for the constraint radius $\delta = 0.2, 0.3$, and 0.4. The differences among them are that the larger the constraint radius is, the longer the time of the recovery is. The magnitude of the constraint radius represents the magnitude of perturbations to the living biomass, the soil moisture and the wilted biomass, which could stand for some types of anthropogenic influences and natural factors, such as grazing, utilization of both surface and underground water resources, fire, etc.. When the constraint radius is large enough, such as $\delta = 0.49$, the ecosystem will shift from the grassland state to the

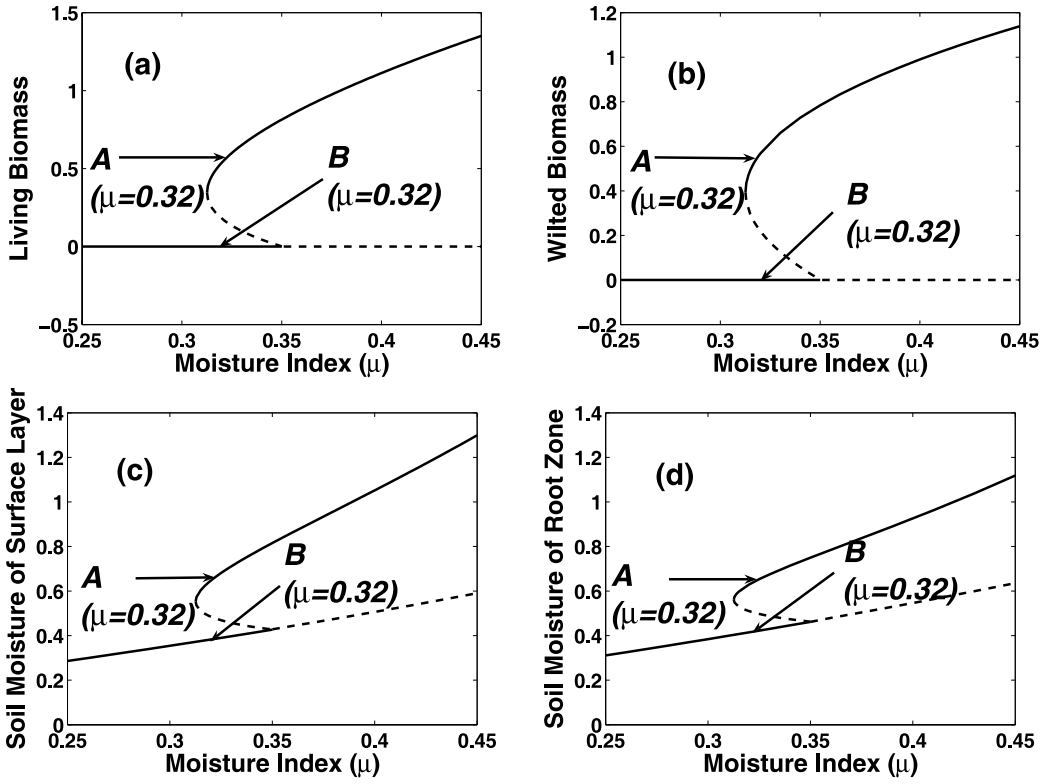

Fig. 1. The equilibrium state of five-variable model as a function of the moisture index, μ. Solid and dashed lines refer to linearly stable and linearly unstable equilibrium states respectively, (a) the living biomass, (b) the wilted biomass, (c) the soil moisture of surface layer, (d) the soil moisture of root zone.

Table 1. The CNOPs and LSVs for the equilibrium state A.

δ	T	CNOPs ($\times 10^{-2}$)	LSVs ($\times 10^{-2}$)
0.005	1	(−0.266, −0.038, −0.245, −0.344)	(−0.265, −0.038, −0.245, −0.343)
0.005	5	(−0.261, −0.034, −0.221, −0.363)	(−0.260, −0.035, −0.222, −0.363)
0.005	10	(−0.261, −0.035, −0.221, −0.363)	(−0.260, −0.035, −0.222, −0.363)
0.2	10	(−11.874, −1.217, −8.196, −13.873)	(−10.408, −1.385, −8.872, −14.527)
0.3	10	(−19.349, −1.677, −11.557, −19.729)	(−15.612, −2.077, −13.308, −21.790)
0.4	10	(−29.868, −1.905, −13.336, −22.944)	(−20.817, −2.769, −17.744, −29.054)
0.49	10	(−47.166, −0.964, −6.540, −11.516)	(−25.518, −3.390, −21.724, −35.587)

desert state, and the transition occurs. In a general way, the larger the negative perturbation of the living biomass, the soil moisture of the surface layer and root zone, and the wilted biomass are, the more unstable the grassland ecosystem is.

To analyze the nonlinear feature of the transition from the grassland state to the desert state, the LSVs are also obtained by maximizing a modified version of J, which is obtained by replacing M in J by its tangent linear approximation (Mu and Zhang, 2006). The results of LSVs are shown in Table 1. It is clear that when the initial perturbation is sufficiently small and the time period is not too long, the patterns of CNOPs are similar to those of LSVs, and for larger initial perturbation and longer time period, there exist considerable differences in nonlinear evolutions between CNOPs and LSVs (Figs. 2 and 3). For $\delta = 0.49$, CNOPs could lead to the transition from the grassland state to the desert state. However, there is no transition caused by the LSVs. These facts demonstrate that the LSVs are more stable than the CNOPs for the equilibrium state A under the condition of $\delta = 0.49$, and the transition exhibits the nonlinear feature.

The main difference between the five-variable and the three-variable models is that the soil layer being divided into the surface layer and root zone. One of the advantages of this division is that the change of the moisture in the surface layer provide a signal of transition earlier than the one in the whole soil layer. To demonstrate this, we investigate the

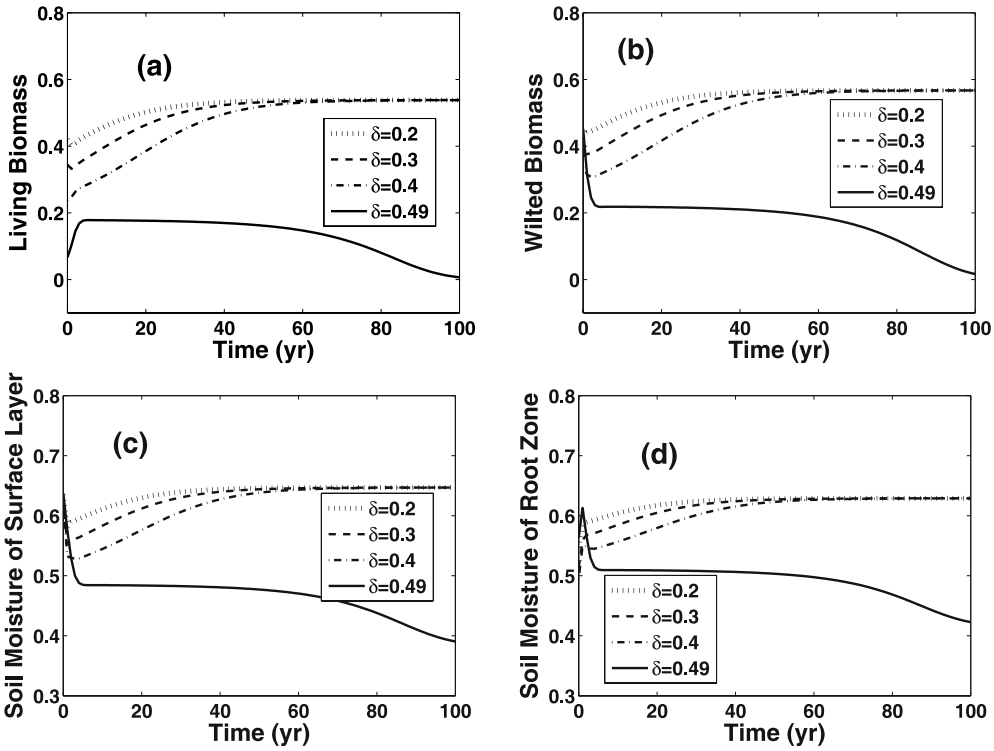

Fig. 2. The 100-year nonlinear evolutions of the grassland ecosystem for different values of δ, with grassland state A plus CNOPs as initial values. (a), (b), (c) and (d) are the same as Fig. 1.

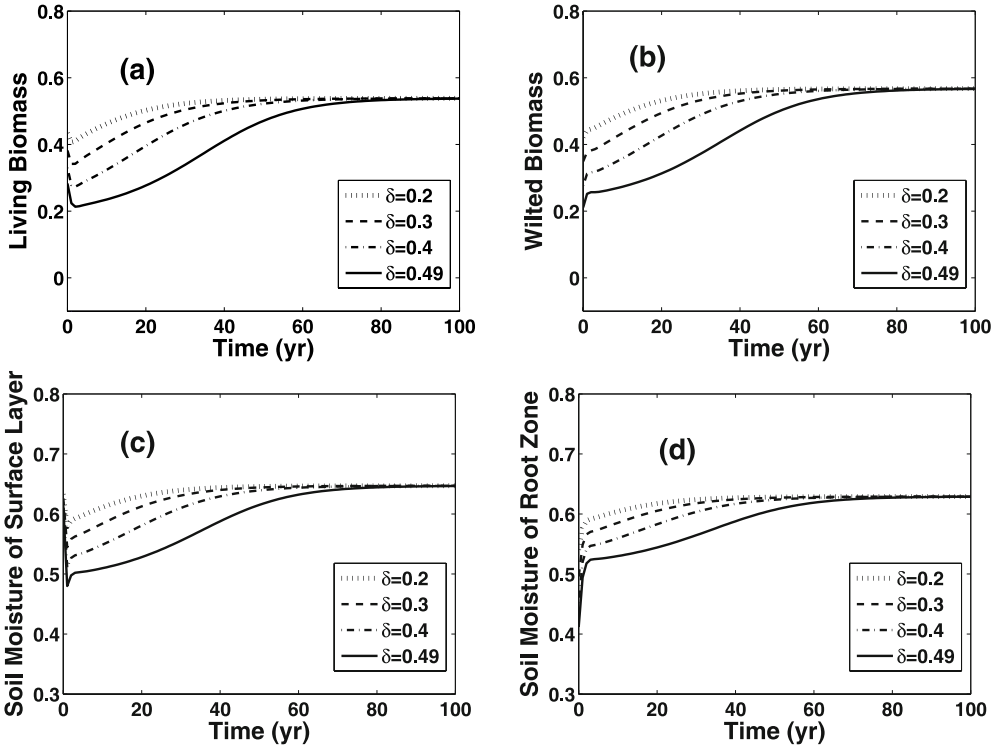

Fig. 3. The same as Fig. 2, but with grassland state A plus LSVs as initial values. (a), (b), (c) and (d) are the same as Fig. 1.

soil moisture in the surface layer and the root zone, whose rate of change with $dx/dt, dy_1/dt, dy_2/dt$ and dz/dt are calculated when the transition occurs. At initial time, $dx/dt > 0, dy_1/dt < 0, dy_2/dt > 0$ and $dz/dt < 0$ when δ=0.49. It is found that the changes of soil moisture in the surface layer and the root zone are different at initial time. The former decreases, while the latter increases. After one year, the former keeps on decreasing, and the latter begins to decrease, i.e., $dy_1/dt < 0, dy_2/dt < 0$. The transition from the grassland state to the desert state occurs when the moisture of the two layers gradually decreases. In Mu and Wang's work (2007), they find that $dx/dt > 0, dy/dt > 0$ and $dz/dt < 0$ where y is the soil moisture of the whole layer. It is clear that the model used in this paper provides a visible signal of the transition, while the three-variable model does not give such a signal (Mu and Wang, 2007).

Zeng et al. (2004) emphasized the shading effect of the wilted biomass in the semi-arid region. The results of Mu and Wang (2007) also supported this point of view with the three-variable ecosystem model. For the five-variable ecosystem model, the contrast of nonlinear evolutions between the CNOPs and the perturbation of ($-\delta$, 0, 0, 0) shows that the shading effect of the wilted biomass is important for the grassland ecosystem, since the negative perturbation to the living biomass will not make the transition occur for $\delta = 0.49$ and $\mu = 0.32$. Meanwhile, the magnitude of CNOPs to the wilting biomass is 0.115, which is approximately 5.5% of that of the constraint radius $\delta = 0.49$.

3.2 *Nonlinear stability analysis of desert state B*

CNOPs are calculated to analyze the stability of the desert equilibrium state B (Table 2). The nonlinear evolutions of the ecosystem with desert state B plus CNOPs as initial values are presented in Fig. 4.

Figure 4 shows that the nonlinear evolutions are different between $\delta = 0.1$ and 0.2. The larger the constraint radius, the longer the time of recovering to the equilibrium state B. The constraint radius represents magnitude to the living biomass, the soil moisture and the wilted biomass, which represent some kind of anthropogenic influences and natural factors, such as planting and irrigation etc. When $\delta = 0.3$ and 0.4, the nonlinear evolutions of the ecosystem change essentially. The desert state B shifts to the grassland state A. This means that the desert state B is nonlinearly unstable to large enough positive perturbation, such as planting and irrigation.

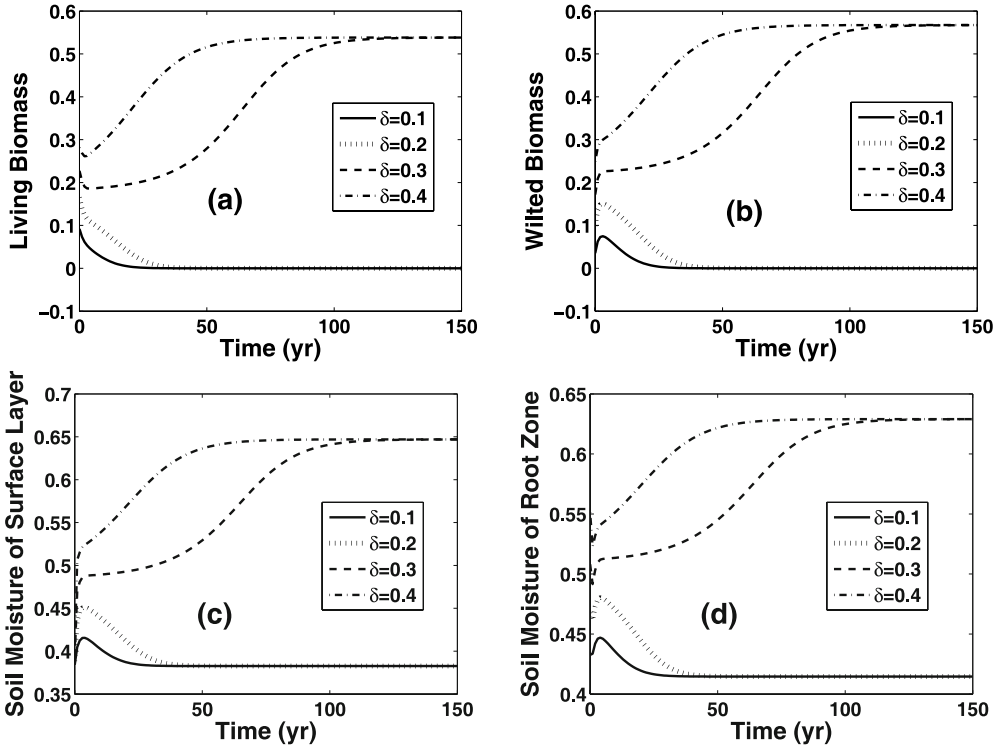

Fig. 4. The 150-year nonlinear evolutions of the desert ecosystem for different values δ, with desert state B plus CNOPs as initial values. (a), (b), (c) and (d) are the same as Fig. 1.

Table 2. The CNOPs and LSVs for the equilibrium state B.

δ	T	CNOPs ($\times 10^{-2}$)	LSVs ($\times 10^{-2}$)
0.005	1	(0.396, 0.004, 0.031, 0.304)	(0.398, 0.004, 0.029, 0.302)
0.005	5	(0.490, 0.000, 0.005, 0.101)	(0.491, 0.000, 0.000, 0.094)
0.005	10	(0.498, 0.000, 0.006, 0.040)	(0.499, 0.000, 0.000, 0.029)
0.1	10	(9.184, 0.212, 1.760, 3.537)	(9.983, 0.000, 0.000, 0.586)
0.2	10	(16.556, 0.652, 5.256, 9.892)	(19.965, 0.000, 0.000, 1.172)
0.3	10	(22.727, 1.195, 9.310, 17.187)	(29.948, 0.000, 0.000, 1.758)
0.4	10	(28.117, 1.811, 13.622, 24.912)	(39.931, 0.000, 0.000, 2.344)

To analyze the nonlinear feature of the transition from the desert state B to the grassland state A, the LSVs are calculated (Table 2). The method is similar to that of the equilibrium state A. It is shown that the patterns of the CNOPs are similar to those of the LSVs in the case of smaller perturbation and shorter time period. The nonlinear evolutions of the equilibrium state B plus LSVs are plotted in Fig. 5. The results show the nonlinear feature of the transition for the desert state B. The CNOPs could lead to the transition from the desert state to the grassland state for δ= 0.3 and 0.4, but no transition occurs for LSVs. The results show that the LSVs are more stable than the CNOPs for the desert state when $\delta = 0.3$ and 0.4.

It is shown in the above subsection that for the grassland state, the soil moisture of the surface layer provides a visible signal of transition when the transition occurs. The same thing also happens to the desert state B. To investigate the changes of soil moisture of different layers, $dx/dt, dy_1/dt, dy_2/dt$ and dz/dt are calculated when the transition from the desert to the grassland occurs. At initial time, $dx/dt < 0, dy_1/dt > 0, dy_2/dt < 0$ and $dz/dt > 0$ for δ=0.3 and 0.4. The soil moisture of the surface layer increases, while the soil moisture of the root zone decreases at initial time. After four years, both of them will increase, i.e., $dy_1/dt > 0, dy_2/dt > 0$. Compared with $dx/dt < 0, dy/dt < 0$ and $dz/dt > 0$ (Mu and Wang, 2007), it is also clear that the five-variable model provides a visible signal of the transition. However, there

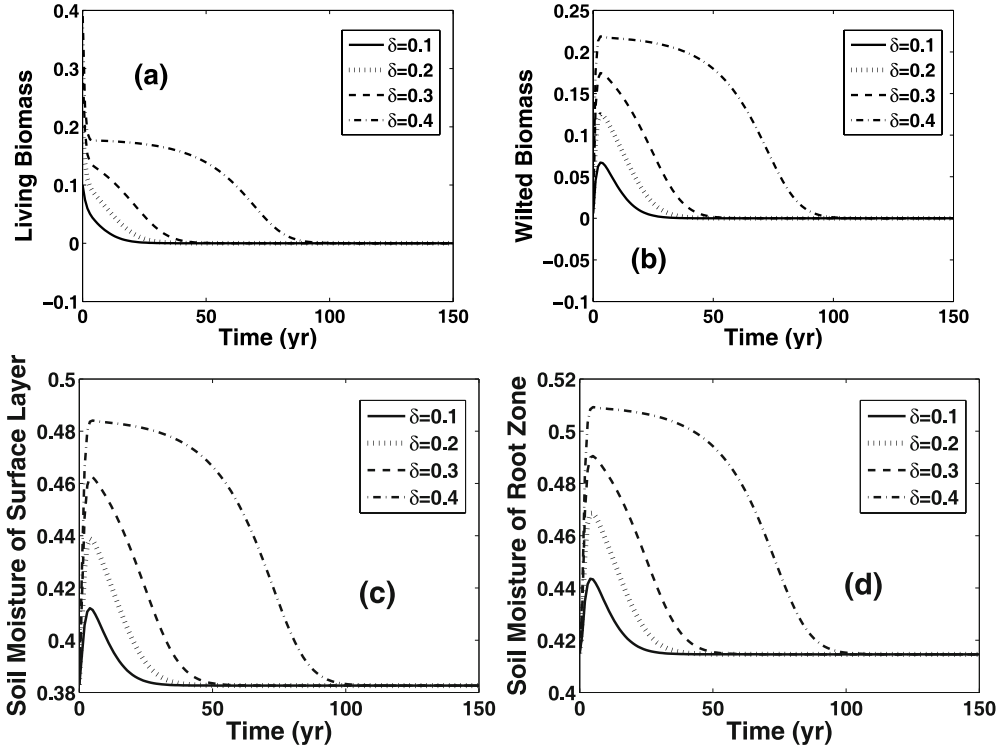

Fig. 5. The same as Fig. 4, but with desert state B plus LSVs as initial values. (a), (b), (c) and (d) are the same as Fig. 1.

is no signal in the three-variable model.

In addition, to consider the shading effect of the wilted biomass for the desert state B, the positive perturbation to the living biomass introduced is adopted (Mu and Wang, 2007). It is shown that the positive perturbation will not induce the transition from the desert state to the grassland state with $\delta = 0.3$ and 0.4 as the five-variable model does (Fig. 6b). The analysis shows that the desert state will not lead to the grassland state for $\mu = 0.32$ when there is no perturbation (introduced perturbation), or only a small perturbation (LSVs, Table 2), to the wilting biomass, and a large enough perturbation to the living biomass. So, when the transition occurs from the desert state to the grassland state, the living biomass is indispensable, whose magnitude is approximately 49.4% of that of the constraint radius ($\delta = 0.4$) for CNOPs. At the same time, the magnitude of perturbation to the wilted biomass, 0.249 for CNOPs, is very important and has a nonlinear influence on the transition.

3.3 *The result obtained by Lyapunov vectors*

To further analyze the stability of the ecosystem and the nonlinear feature of the transition, we also show the result obtained by the Lyapunov vectors (LVs) which represents the direction in which maximum sustainable growth can occur for an infinitely long optimization time period. The method to calculate the Lyapunov exponent and its vector was introduced by Wolf et al. (1985). The details that show how to calculate the LVs can also be found in Kalney (2003) or Appendix B.

To identify the similarities and the differences among CNOPs, LSVs and LVs, the same constraint radii are chosen. The results of LVs are (-0.065, -0.031, -0.021, -0.066) for the grassland state A and (0.024, 0.039, 0.040, 0.079) for the desert state B respectively when $\delta = 0.1$. For other δ, LVs can be obtained by multiplying them with a proper factor according to the linear characteristic. Also, the direction of the LVs is independent of δ. The equilibrium states A and B plus the corresponding LVs are integrated respectively. The results show that the LVs could not lead to the transition like LSVs for the same constraint radius (Fig. 7). However, the time of the equilibria state recovering for the LVs is shorter than that for the LSVs. So, the LVs are more stable than the LSVs.

3.4 *The case of other moisture index*

To confirm the consistency of the moisture index, the results of the moisture index $\mu = 0.325$ are also shown. Here, two different equilibrium states C ($x =$

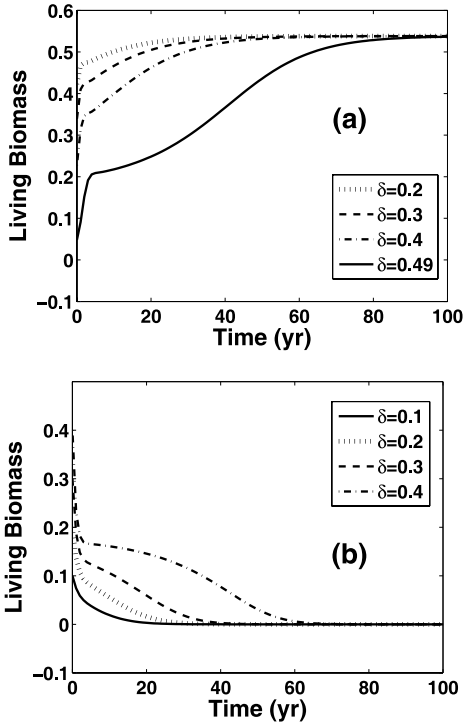

Fig. 6. The evolution of only negative perturbation to living biomass. (a) for grassland equilibrium state $(-\delta, 0, 0, 0)$; (b) for desert equilibrium state $(\delta, 0, 0, 0)$.

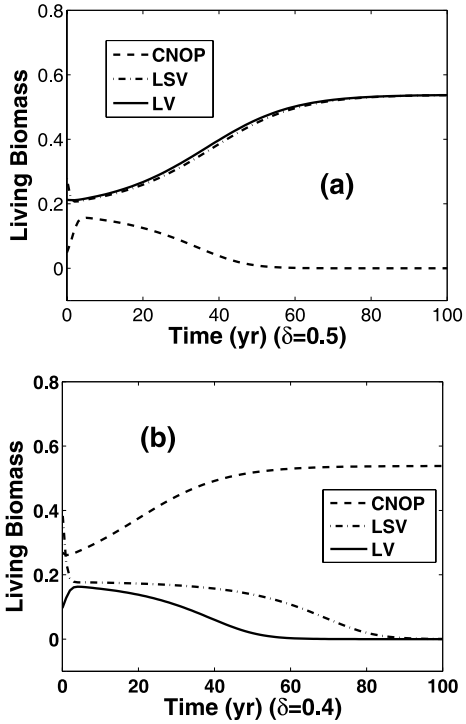

Fig. 7. The comparison of evolution among CNOPs, LSVs and LVs in the living biomass. (a) for grassland equilibrium state; (b) for desert equilibrium state.

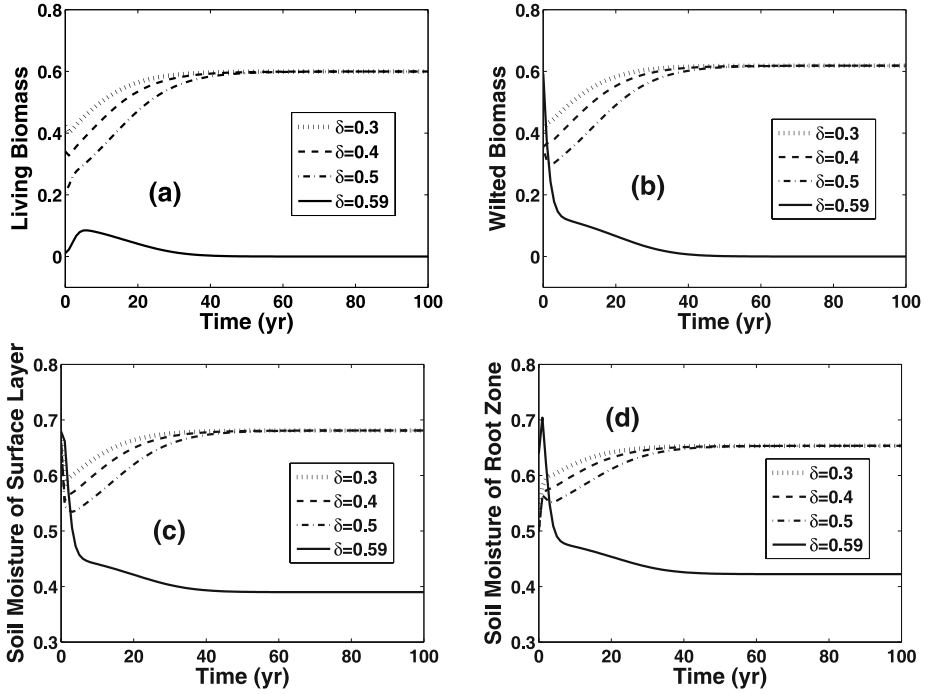

Fig. 8. The same as Fig. 2, but for $\mu = 0.325$. (a), (b), (c) and (d) are the same as Fig. 1.

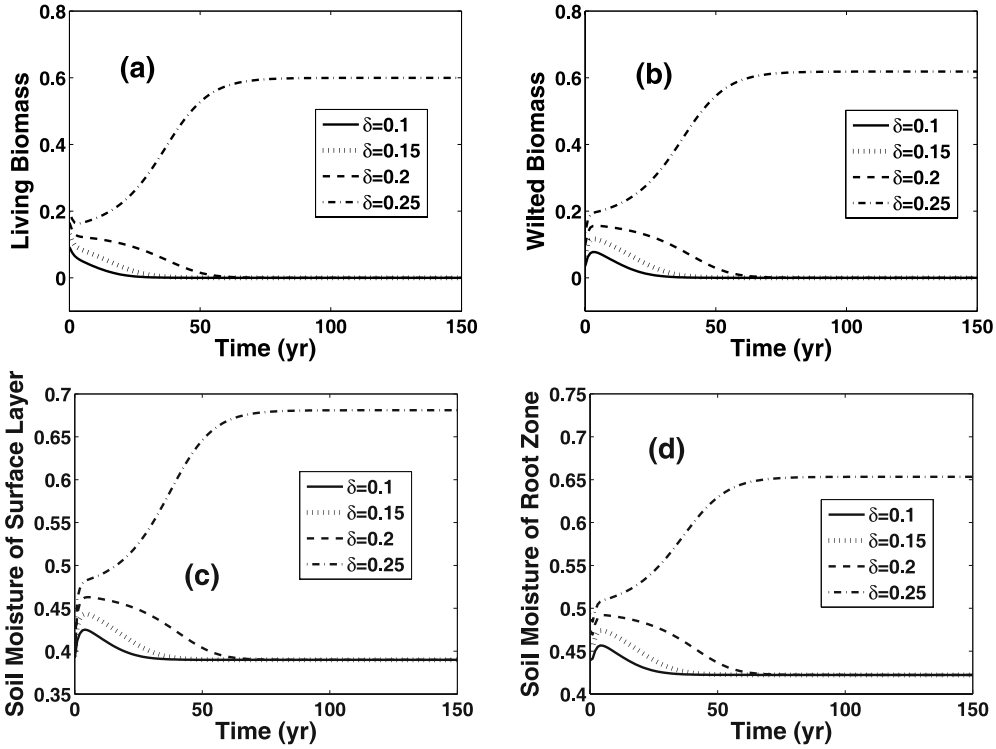

Fig. 9. The same as Fig. 4, but for $\mu = 0.325$. (a), (b), (c) and (d) are the same as Fig. 1.

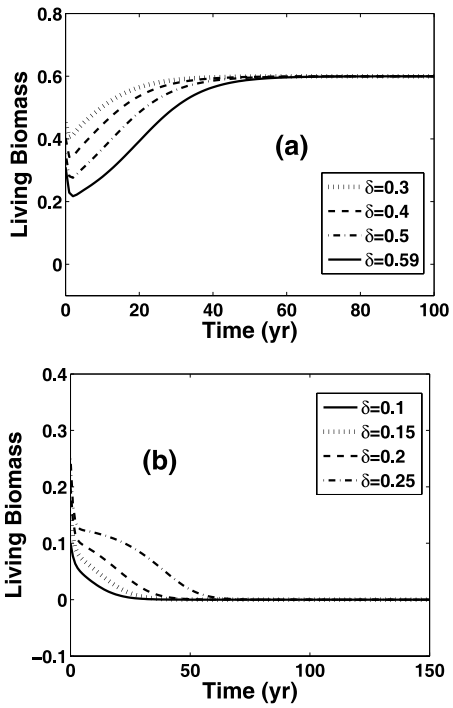

Fig. 10. The evolution of LSVs plus equilibrium states for living biomass as $\delta = 0.325$. (a) for grassland equilibrium state A; (b) for desert equilibrium state B.

0.600, $y_1 = 0.681, y_2 = 0.653, z = 0.619$) and D ($x = 0.000, y_1 = 0.390, y_2 = 0.422, z = 0.000$) are chosen.

For the moisture index $\mu = 0.325$, there are similar results in the stability of equilibrium state (Figs. 8 and 9) and the nonlinear feature of the transition (Fig. 10). The numerical results also show the visible signal in the soil surface layer and the nonlinear shading effect of the wilting biomass. However, there are some differences between the results for the two different moisture indexes. For the transition from the grassland state to the desert state, the larger the moisture index, the more difficulty the transition and the more stable the grassland state. When the moisture index is 0.325 and the transition occurs, the magnitude of the perturbation accounts for 99.7% of that of all perturbation ($\delta = 0.59$) to the living biomass, while 92.7% of $\delta = 0.49$ for $\mu = 0.32$. On the other hand, for the transition from the desert state to the grassland state, the larger the moisture index, the easier the transition is and the more unstable the desert state is. The transition occurs for $\mu = 0.325$ when the constraint radius is 0.25, while it does not occur for $\mu = 0.32$.

4. Summary and discussion

Based on the five-variable ecosystem model, we analyze the stability of the ecosystem and the nonlinear

feature of the transition between the grassland and the desert states.

It is shown that the linearly stable grassland and desert states are nonlinearly stable to small initial perturbations, while the states are nonlinearly unstable to large enough anthropogenic influence and natural factors according to the theoretical model, when the moisture index satisfies $\mu_1 < \mu < \mu_2$. Also, there is the nonlinear feature in the transition. For the grassland state A, $\delta = 0.49$, and for the desert state B, $\delta = 0.3, 0.4$, the CNOPs make the transitions occur, but the LSVs and the LVs fail for the same finite amplitude perturbation.

In the five-variable model, the soil layer is divided into the surface layer and root zone, which is different from the three-variable model. By comparing the change of every variable, it is found that the changes of soil moisture are different in the two layers at initial time. $dy_1/dt < 0$ and $dy_2/dt > 0$ for the grassland state, and $dy_1/dt > 0$ and $dy_2/dt < 0$ for the desert state. When the time increases, $dy_1/dt < 0$ and $dy_2/dt < 0$ for the grassland state, and $dy_1/dt > 0$ and $dy_2/dt > 0$ for the desert state. Then, the transitions occur. The five-variable model is able to provide a visible signal of the transitions. However, the signal does not appear in the three-variable ecosystem model.

The shading effect of the wilted biomass has important nonlinear influence on the ecosystem. For the grassland equilibrium state, the perturbation to the wilted biomass could make the transition occur from the grassland state to the desert state with CNOPs, and has nonlinear influence on the transition. For the desert equilibrium state, the perturbation to the living biomass is indispensable, and the shading effect of the wilted biomass has a nonlinear effect on the transition from the desert state to the grassland state by contrasting the CNOPs and LSVs. So the "shading effect" of the wilted biomass might be a major nonlinear mechanism leading to the desertification (Zeng et al., 2004) second to the albedo mechanism (Charney, 1975).

In the five-variable ecosystem model, the moisture index is an important factor, which is the only external input. The comparison of the results of different moisture indices shows that the better the climate condition is, the more difficult the transition becomes for the grassland state, and the easier the transition becomes for the desert state.

Acknowledgements. The authors thank the reviewers for their valuable suggestions. Funding was provided by grants from the state Key Development Program for Basic Research (Grant No. 2006CB400503), the KZCX3-SW-230 of the Chinese Academy of Sciences (CAS) and National Natural Science Foundation of China (Grant No. 40675030).

APPENDIX A

The Introduction of the Five-Variable Ecosystem Model

In the theoretical ecological-hydrological model, some expressions could refer to Zeng et al. (2004, 2006), and the explanations of the right terms refer to Table A1. In addition, the other four expressions are derived to analyze the stability of the ecosystem.

Firstly, $P_c + P_s + P_r = P, P_c = \min(P_c^*, P), P_s = \min(P_s^*, P - P_c)$, P_c^* and P_s^* are saturated values or the permissibly upper bounds of P_c and P_s respectively, and they depend on the vegetation characteristics and soil properties (Zeng et al., 2003). Here, precipitation is assumed to be constant. It is assumed that

$$0 \leqslant P_c^* < P, \;\; 0 \leqslant P_s^* < P - P_c^* \, ,$$

and P_c^* increases monotonically with M_c:

$$P_c^* = \alpha_c P(1 - e^{-\varepsilon_c \frac{M_c}{\bar{x}}}) \, . \tag{A1a}$$

The expressions of the interception of surface layer and root zone respectively are:

$$P_s^* = \alpha_s (P - P_c^*) \, , \tag{A1b}$$

$$P_r = (1 - \alpha_s)(P - P_c^*) \, . \tag{A1c}$$

It is obvious that the sum of Eqs. (A1a), (A1b) and (A1c) is P. Secondly, the term of runoff R_r is given in the physical hypothesis below. R_r depends on P_r, W_r and M_c. R_r increases monotonically with P_r and W_r, and decreases monotonically with M_c, since the root of the living biomass influences the runoff of the root zone. So R_r is:

$$R_r = \lambda_r P_r (e^{\varepsilon_r \frac{W_r}{y_2}} - 1)[1 - \kappa_r (1 - e^{-\varepsilon_r' \frac{M_c}{\bar{x}}})] \, . \tag{A2}$$

Also, the parameters of the above expressions (A1a, A1b, A1c and A2) are shown in Table A2.

In addition, the depths of the thin surface layer and root zone need to be estimated. It is assumed that the depths of surface layer D_s and root zone D_r are 100 mm and 500 mm respectively. $y_s^*/D_s = y_r^*/D_r$ is satisfied to guarantee the vanishing of the water exchange when the surface layer and root zone are both saturated (Zeng et al., 2005c). y_s^* and y_r^* are field capacities of the surface layer and root zone respectively. $\tilde{y}_1 = 0.5 y_s^*$ and $\tilde{y}_2 = 0.5 y_r^*$ are assumed (Zeng et al., 2004). Then, $\tilde{y}_1/D_s = \tilde{y}_2/D_r$. The characteristic va-

Table A1. The physical explanation of the right term in the five-variable model.

Parameter	The physical explanation
α^*	The maximum growth rate
G	The dimensionless growth of living biomass
D_c	Wilting of living biomass
C_c	Consuming terms of living biomass
$\beta' D_c$	The dimensionless wilting biomass accumulation
D_d	Decomposition of wilted biomass
C_d	Consuming terms of wilted biomass
E_s	The surface evaporation of bare soil
E_r	Vegetation transpiration
P_c	The interception of precipitation (only input) by vegetation canopy layer
P_s	The interception of precipitation by surface layer
P_r	The interception of precipitation by root zone
Q_{sr}	The conductive transport from the surface soil to the root
R_c	The runoff of the canopy layer
R_s	The runoff of the surface layer
R_r	The runoff of the root zone

Table A2. The parameter values in four terms P_c, P_s, P_r and R_r.

Parameter	Value
$\tilde{y}_1$ (mm)	40
$\tilde{y}_2$ (mm)	200
D_s (mm)	100
D_r (mm)	500
α_s	0.9
α_c	0.1
ε_c	1.0
λ_r	0.015
ε_r	1.0
κ_r	0.7
ε'_r	0.7

lue of soil moisture is 240 mm in the study of Zeng et al. (2004, 2005c). Therefore, we assume $\tilde{y}_1 = 40$ mm, $\tilde{y_2} = 200$ mm.

APPENDIX B

Computation of the First Lyapunov Vectors

Because readers may not be familiar with the LVs, we will give a brief introduction on how to calculate the first LVs. Assume that $f(x,t)$ satisfies the equations of a nonlinear model $f(x, t + \triangle t) = M(f(x,t))$, where M is the nonlinear propagator. The linear evolution of a perturbation is shown by $\delta f(x, t + \triangle t) = L(f, t, \triangle t)(\delta f(x,t))$, where $L = \partial M/\partial f$ is the tangent linear model (TLM).

The Lyapunov vector is calculated as follows:

(1) An arbitrary perturbation $\delta f(x,t)$ is given;

(2) Integrate the TLM from t to $t + \Delta t$;

(3) Repeat (2) for the succeeding time intervals.

After a sufficiently long time $t_n = n \triangle t, n \to \infty$, the perturabtion $\delta f(x,t)$ will converge to the first Lyapunov vectors.

REFERENCES

Charney, J. G., 1975: Dynamics of deserts and drought in the Sahel. *Quart. J. Roy. Meteor. Soc.*, **101**, 193–202.

Claussen, M., 1997: Modeling biogeophysical feedback in the Africa and India monsoon region. *Climate Dyn.*, **13**, 247–257.

Claussen, M., 1998: On multiple solutions of the atmosphere-vegetation system in present-day climate. *Global Change Biology*, **4**, 549–559.

Claussen, M., C. Kubatzki, V. Brovkin, A. Ganopolski, P. Hoelzmann, and H. Pachur, 1999: Simulation of an abrupt change in Saharan vegetation in the mid-Holocence. *Geophys. Res. Lett.*, **26**, 2037–2040.

Duan, W. S., M. Mu, and B. Wang, 2004: Conditional nonlinear optimal perturbation as the optimal precursors for El Niño-Southern Oscillation events. *J. Geophys. Res.*, **109**, D23105, doi: 10.1029/2004JD004756.

Kalney, E., 2003: *Atmospheric Modeling, Data Assimilation and Predictability*. University Press, Cambridge, 341pp.

Klausmeier, C. A., 1999: Regular and irregular patterns in semiarid vegetation. *Science*, **284**, 1826–1828.

Li, T., Robert F. Granta and Lawrence B. Flanaganb, 2004: Climate impact on net ecosystem productivity of a semi-arid natural grassland: Modeling and measurement. *Agricultural and Forest Meteorology*, **126**, 99–116.

Liu, Z., Y. Wang, R. Gallimore, M. Notaro, and I. C. prentice, 2006: On the cause of abrupt vegetation collapse in North Africa during the Holocene: Climate variability vs. vegetation feedback. *Geophys.*

Res. Lett., **33**, L22709, doi: 10.1029/2006GL028062.

Mu, M., W. S. Duan, and B. Wang, 2003: Conditional nonlinear optimal perturbation and its applications. *Nonlinear Processes in Geophysics*, **10**, 493–501.

Mu, M., and W. S. Duan, 2003: A new approach to studying ENSO predictability: Conditional nonlinear optimal perturbation. *Chinese Science Bulletin*, **48**, 1045–1047.

Mu, M., and Z. Zhang, 2006: Conditional nonlinear optimal perturbations of a two-dimensional quasi-geostrophic model. *J. Atmos. Sci.*, **63**, 1597–1604.

Mu, M., and B. Wang, 2007: Nonlinear instability and sensitivity of a theoretical grassland ecosystem to finite-amplitude perturbations. *Nonlinear Processes in Geophysics*, **14**, 409–423.

Mu, M., L. Sun, and H. A. Dijikstra, 2004: The sensitivity and stability of the ocean's thermohaline circulation to finite amplitude perturbations. *J. Phys. Oceanogr*, **34**, 2305–2315.

Sitch, S., and Coauthors, 2003: Evaluation of ecosystem dynamics, plant geography and terrestrial carbon cycling in the LPJ Dynamic Vegetation Model. *Global Change Biology*, **9**, 161–185.

Sun, L., M. Mu, D. J. Sun, and X. Y. Yin, 2005: Passive mechanism of decadal variation of thermohaline circulation. *J. Geophys. Res.*, **110**, C07025, doi: 10.1029/2005JC002897.

Wolf, A., J. B. Swift, H. L. Swinney, and J. A. Vastano, 1985: Determining Lyapunov exponents from a time series. *Physica*, **16D**, 285–317.

Zeng, N., 2003: Drought in the Sahel. *Science*, **302**, 999–1000.

Zeng, N., K. Hales, and J. D. Neelin, 2002: Nonlinear dynamics in a coupled vegetation-atmosphere system and implications for desert-forest gradient. *J. Climate*, **15**, 3474–3487.

Zeng, Q. C., P. S. Lu, and X. D. Zeng, 1994: Maximum simplified dynamic model of grass field ecosystem with two variables. *Science in China B*, **37**, 94–103.

Zeng, Q. C., and X. D. Zeng, 1996a: An analytical dynamic model of grass field ecosystem with two varibles. *Ecological Modelling*, **85**, 187–196.

Zeng, Q. C., and X. D. Zeng, 1996b: Two-variable dynamic model of grass field ecosystem with seasonal variation. *Ecological Modelling*, **85**, 197–202.

Zeng, Q. C., X. D. Zeng, A. H. Wang, R. E. Dickinson, X. B. Zeng, and S. S. H. Shen, 2003: Models and numeraical simulation of atmosphere-vegetation-soil interactions and ecosystem dynamics. *Proceedings of ICCP6-CCP2003*, Rinton Press Inc., Beijing, 18pp.

Zeng, X. D., S. S. P. Shen, X. B. Zeng, and R. E. Dickinson, 2004: Multiple equilibrium states and the abrupt transitions in a dynamical system of soil water interacting with vegetation. *Geophys. Res. Lett.*, **31**, 5501, doi: 10.1029/2003GL018910.

Zeng, Q. C., X. D. Zeng, A. H. Wang, R. E. Dickinson, X. B. Zeng, and S. S. H. Shen, 2005a: Some studies of the hydrological interactions in the atmosphere-ecosystem-soil system. *Chinese J. Atmos. Sci.*, **29**(1), 7–19. (in Chinese with English abstract)

Zeng, X. D., A. H. Wang, G. Zhao, S. S. P. Shen, X. B. Zeng, and Q. C. Zeng, 2005b: Ecological dynamic model of grassland and its practical verification. *Science in China*(*C*), **48**, 41–48.

Zeng, X. D., X. B. Zeng, S. S. P. Shen, R. E. Dickinson, and Q. C. Zeng, 2005c: Vegetation-soil water interaction within a dynamical ecosystem model of grassland in semi-arid areas. *Tellus*, **57B**, 189–202.

Zeng, X. D., A. H. Wang, Q. C. Zeng, R. E. Dickinson, X. B. Zeng, and S. S. H. Shen, 2006: Intermediately complex models for the hydrological interactions in the atmosphere-vegetation-soil system. *Adv. Atmos. Sci.*, **23**(1), 127–140.